Irreversibility of dislocation motion under cyclic loading due to strain gradients

Markus Stricker[a], Daniel Weygand[a,*], Peter Gumbsch[a,b]

[a] *Karlsruhe Institute of Technology IAM, Kaiserstraße 12, 76131 Karlsruhe, Germany*
[b] *Fraunhofer IWM, Woehlerstr. 11, 79108 Freiburg, Germany*

Abstract

Mechanisms that make dislocation motion irreversible are associated with the formation of dislocation junctions and cross-slip, leaving dislocations trapped inside the specimen. Using Discrete Dislocation Dynamic simulations, we identify another mechanism that produces irreversible plastic deformation and leaves no or only very few dislocations inside the sample: Under cyclic loading, dislocations which pass the neutral plane during loading (pile-up formation), generate a slip step upon unloading. The explanation is an intrinsic asymmetry between the backward and forward motion. An additional bias may be introduced by the geometry of the specimen due to the shortening of the line length of dislocations.

Keywords: irreversibility, plasticity, dislocation structure, bending, torsion

Irreversible plasticity is associated with the glide and storage of dislocations through multiplication under load by dislocation junction formation [1, 2, 3] or absorption of dislocations in grain boundaries [4]. For bulk-like fcc materials under fatigue conditions, complex dislocation microstructures develop consisting of veins and almost dislocation free channels [5]. These dislocation microstructures lead to the surface roughness and finally to failure due to crack growth [6, 7, 8]. On the other hand, specimens with a thickness less than a few micrometers, e.g. thin metallic films, have a higher fatigue resistance, as the formation of extrusions and intrusions is reduced by the confinement of the dislocation glide

*Corresponding author
Email address: daniel.weygand@kit.edu (Daniel Weygand)

within the much smaller structure [9].

Recent investigations of the fatigue behavior of single crystalline microbeams with thicknesses of ≈ 2 and $\approx 10\,\mu$m under cyclic bending show the development of slip traces on the surface, generated by dislocations leaving the specimen [10]. The normalized stress versus displacement plot shows a clear Bauschinger effect, which is also observed in the complementary Discrete Dislocation Dynamics (DDD) simulations [10]. The origin of the Bauschinger effect in this case is the specific dislocation arrangement, found to be typical for bending: Dislocations cross the neutral plane and form a symmetric pile-up around the neutral axis [11]. The internal stress gradient stabilizes the dislocation pile-up within the specimen [11, 12, 13]. From more recent experimental measurements, by Laue diffraction, the formation of geometrically necessary dislocations (GND) arrangements is reported, compatible with the formation of the pile-ups around the neutral plane [14]. These GNDs disappear upon unloading, but the amount of permanent plastic deformation and the evolution of the pile-up during unloading is less clear. Upon unloading, it is suggested that dislocations move towards both surfaces [10, 14], which leads to an irreversible plastic deformation. The Bauschinger effect is in general attributed to the dissolution of pile-ups of dislocations in front of interfaces or dissolution of dislocation cells during reverse loading [15]. Several studies with DDD have addressed the question of reversibility of dislocation motion and its conditions in detail, e.g. [16, 17, 18]. The current study does not consider the role of strong fixed obstacles on dislocation glide. The focus is on inhomogeneous loading conditions, e.g. bending or torsion, where the imposed stress gradients inhibit dislocation motion within the volume during loading. These imposed gradients vanish gradually upon unloading. While the formation of pile-ups in bending loading conditions is well documented [10, 11, 13, 14, 19], the evolution of the dislocation microstructure upon unloading has not yet been studied in detail especially in the limit of a very low dislocation density, e.g. for individual pile-ups. Neither has a generalization to other gradient-type loading conditions (e.g. torsion) been attempted yet.

Therefore the focus in this study is on the properties of a minimal setup showing irreversible plastic deformation under cyclic loading involving both macroscopic strain gradients – as a consequence of boundary conditions – and the shape of the specimen. The set-up mimics the situation in small micrometer-sized samples with a low number of activated dislocations sources. Cross-slip of screw dislocations as a possible additional source of irreversibility is not allowed. The DDD code described in [20, 21, 22] is used for this study. Dislocations are represented by nodal points, connected by straight segments. Nodal forces are calculated from the resolved Peach-Koehler force acting along the segments. Boundary conditions, finiteness of the specimen and image forces are included following the superposition scheme [23]. As a model system, material parameters for aluminum are used assuming isotropic elasticity (lattice parameter $a = 0.404\,\mathrm{nm}$, shear modulus $G = 27\,\mathrm{GPa}$, Poisson's ration $\nu = 0.347\mathrm{m}$, fcc glide systems). The single crystalline specimen has a quadratic cross section (x-z plane) with a side length (thickness) of $1.5\,\mu\mathrm{m}$ and an aspect ratio of 3. The long axis is along the y-direction. Cross-slip is not activated in this study.

Figure 1 shows the dislocation source positions for both setups. In case of bending, the source is of edge type; the torsion setup has a screw type source. If not specified otherwise, the boundary conditions are:

- **Pure Bending:** Load is applied by prescribing a moment around the z-axis, prescribing displacements at y_{min} and y_{max} [11]. The tensile stress component in y-direction is balanced to be zero by adapting the displacement in y-direction of the beam at the neutral plane at the face y_{max}. All other faces have traction free boundary conditions.
  One load cycle consists of a linear load increase to a maximum normalized displacement (normalized by beam thickness $t = 1.5\,\mu\mathrm{m}$) $u_{\mathrm{norm}} = 0.6\,\%$, and subsequent unloading to $u_{\mathrm{norm}} = 0\,\%$.

- **Torsion:** Loading is applied by fixing all displacement components of the lower face to zero ($u_x = u_y = u_z = 0$) and rotating the upper face in clockwise direction around the torsion axis (parallel to the y-direction)

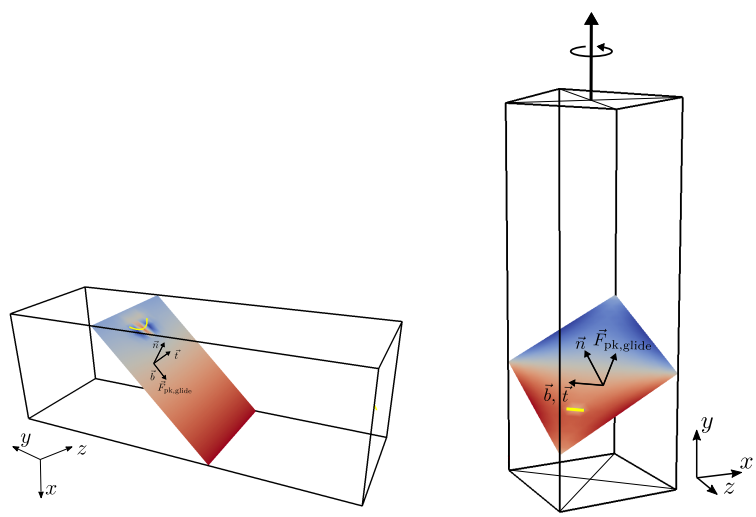

(a) Pure bending case.

(b) Torsion case.

Figure 1: Dislocation source positions for both loading conditions: (a) pure bending and (b) torsion. The glide plane is colored using the resolved shear stress (qualitatively) acting on the dislocation, characterized by its Burgers vector $\vec{b}$, glide plane normal vector $\vec{n}$ and initial line direction $\vec{t}$.

using a torsion rate of $\dot{\varphi} = 3\,^\circ\mu\mathrm{s}^{-1}$ during loading as described in [24]. Traction free boundary conditions are assumed for all other degrees of freedom on the surface. One load cycle consists of a linear loading up to a maximum torsion angle of $\varphi = 1.7\,^\circ$ and a linear unloading part back to $\varphi = 0\,^\circ$ with the same rate.

The shear stresses acting on the used glide systems of the two setups are shown in Fig. 1. Both show a change in sign of the resolved shear stress (indicated by a change from blue to red). The zero-stress plane (neutral plane) spans through the whole specimen and only the cut with the glide plane is visible. In case of bending the neutral plane has a normal vector parallel the x-direction. For torsion, the neutral plane has a normal parallel to the sample cross-section diagonal $(10\bar{1})$.

Figure 2 gives a two dimensional representation of the bending beam of Figure 1(a). In this gradient setting, the dislocations take stable position according to a equilibrium between the stress induced by the bending boundary condition and the growing back stress of the dislocation pile-up [11, 13]. The dashed grey line indicates the neutral plane. Dislocation positions before, during and after the maximum applied bending moment $M_{\mathrm{B,max}}$ of one load-unload cycle are shown: the positions before the maximum moment are colored in red. An increase in load to $M_{\mathrm{B,max}}$ pushes the dislocations further into the center of the beam (black positions). Upon unloading (blue positions and arrows indicating motion), the dislocations, which have crossed the neutral plane, move to the opposite side of the source and leave the volume. The ones, which did not cross, leave on the source side, if they succeed to cross the source location.
This process is repeatable. In the next load cycle, further dislocations are emitted from the source and upon unloading, the ones, which crossed the neutral plane, leave the specimen on the side opposite to the source, creating a slip trace of increasing height on the surface with increasing number of cycles.

For the torsion specimen, the torsion angle is increased until one dislocation passes the neutral plane (Fig. 3 (a), indicated by arrows). Dislocations leave

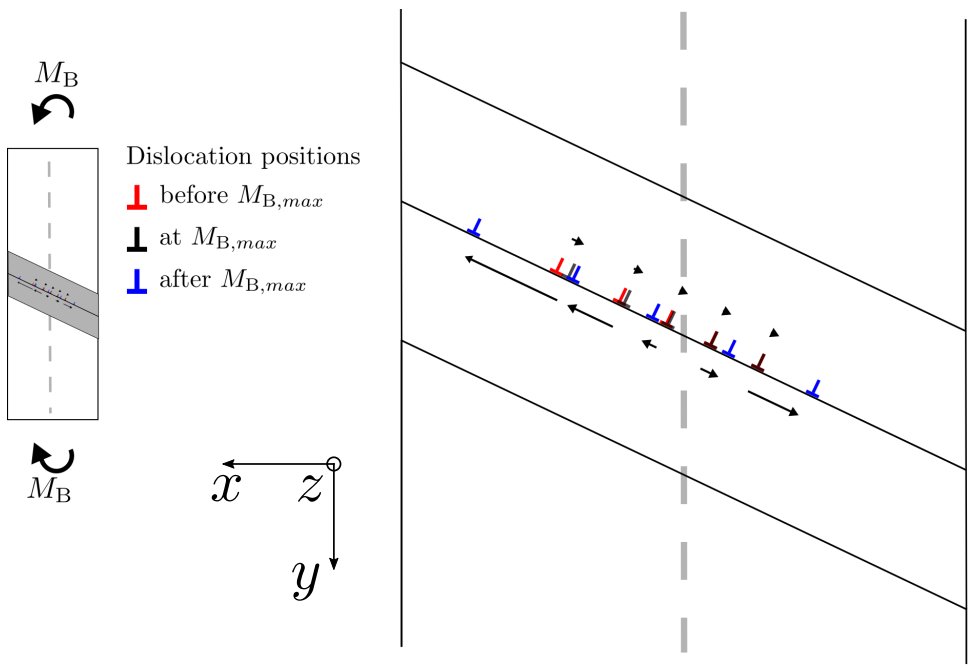

Figure 2: Pure bending: 2D representation of Figure 1(a): Dislocation position before, at and after $M_{\mathrm{B,max}}$ under pure bending. Small figure with the beam indicates the position of the glide plane. The neutral plane is indicated by the grey dashed line. Arrows indicate the position change of dislocations from state to state.

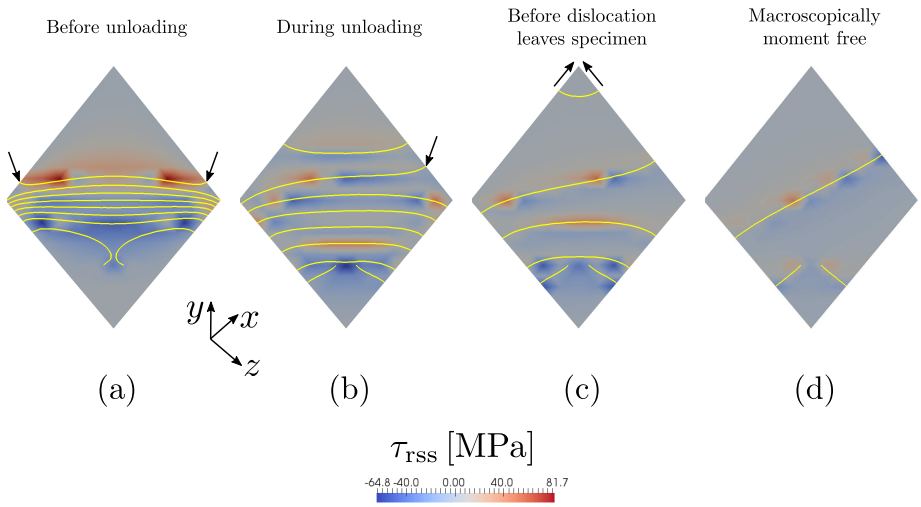

Figure 3: Torsion loading condition: Time series of of the glide plane of the dislocation source during unloading. (a) maximal torsion angle; (b) during unloading; (c) further unloading, right before the dislocation leaves the specimen on the opposite side of the source; (d) complete unloading specimen (macroscopically moment free). The coloring of the plane is according to the resolved shear stress τ_{rss}.

the volume almost orthogonal to the surface, due to image forces. During unloading, a second dislocation passes the neutral plane, but only on the right side (Figure 3 (b)). Further unloading dissolves the pile-up around the neutral plane, but the dislocation which has already passed the neutral plane leaves the volume on the opposite side of the source (Fig. 3 (c)). In the macroscopically moment free state, the dislocation which has passed the neutral line only half, remains blocked inside the volume (Fig. 3 (d)). By evaluating the plastic displacement after unloading, a step is left at the surface of the pillar, caused by the dislocation which crossed the sample.

These two examples show that irreversible plastic deformation occurs in specimens in just one load-unload cycle involving only stress gradients and no formation of dislocation networks or other dislocation reactions, e.g. by cross-slip or junction formation. Common to both scenarios is the initial stabilization of a pile-up within an imposed stress gradients. Once the stress gradient is reduced,

the dislocations having passed the neutral plane experience a lower externally applied shear stress, thus they are pushed further over the neutral plane, due to dislocation-dislocation interaction. The other dislocations, located between source and neutral plane, reverse their glide motion, as the stresses due to dislocation-dislocation interaction within the pile-up is opposed to the applied shear stress.

The pile-up can be simplified to a one dimensional simulation of edge dislocations in a stress gradient: this systems shows a symmetric dissolution of the pile-up upon decreasing the load with respect to the neutral plane, for a fixed number of edge dislocation, avoiding the asymmetry due to the presence of a dislocation source. In case of an even number of edge dislocations, both leave the volume on opposite sides, thus leaving a step of height b. In case of an odd number, the middle dislocation remains in the neutral plane. Although this scenario is highly artificial, it displays the essence that unloading or reversal of a strain gradient leads to some forward dislocation motion and net plastic deformation and not to perfectly reversible dislocation motion. In more realistic situations, both the plastic response from dislocation glide and the presence of a dislocation source will introduce a natural asymmetry even in the simplest scenario studied here since all dislocations start from the source and the local boundary conditions will not remain symmetrical. Which means that the source itself will induce the asymmetry and present an obstacle for the backward motion of the dislocations during unloading. During the backward motion, the source may block the easy way back while the oppositely oriented gradient from the bending boundary condition is of course eliminated by unloading.

A further bias in the glide motion is introduced by the sample geometry and the glide plane orientation with respect to the sample: in the studied torsion setup, it is energetically more favorable for the dislocation to leave the volume on the opposite side of the source, as the dislocation length and therefore its elastic energy decreases when moving in that direction. When the pile-up is dissolved and the macroscopic twist vanishes, the resolved shear stress on the glide plane at the top most dislocation is approximately zero (cf. Figure 3 (c), grey coloring

of glide plane around dislocation). The first dislocation in the pile-up leaves the specimen on the opposite side, all other but one move back and their generated plasticity is reversed. It is important to note that it requires the interaction of two or more dislocations within a stress gradient to push one dislocation beyond the neutral line. Consequently, the observed irreversible dislocation motion can only occur if a dislocation source has produced more than one dislocation.

By looking at the angle at which the dislocations leave the specimen close to the neutral plane (cf. Figure 3 (a,b), arrows), one might argue that forward motion of dislocations pushed over the plane after unloading is a consequence of the square cross section geometry, changing the evolution of the line length of the dislocation once it passes the neutral plane. And although it is harder for a dislocation to glide back over the neutral plane, it can also be argued that it is also harder to push a dislocation over the neutral plane. The reduction of line length does indeed provide another driving force but is by no means restricted to the square cross section specimen geometry used here. For a round cross section the dislocation motion over the neutral plane as well as the motion back is easier, because the change in angle and the line length changes are less pronounced than for the square cross section. Still, the line length also favors further motion of the dislocation beyond the neutral plane, once the dislocation has crossed it.

Both, the line length decrease and the associated energy decrease and the resolved shear stress changes upon unloading favor the same behavior: the complete crossing of the specimen by a dislocation after it has overcome the neutral plane. The crossing is only observed after unloading and the dislocation is not stored in the volume. This means that there is forward plastic flow during unloading, thus the unloading curve might even be steeper than the elastic slope. Experimentally, a Bauschinger effect is also observed on the moment vs. displacement curves [10, 14]. It is connected with a reversible peak broadening in the Laue diffraction patterns [14]. The formation and dissolution of pile-ups towards both directions as described above, is one possible mechanism to explain such behavior. The symmetry of the pile-up evolution might be changed

by cross-slip or junction formation, blocking dislocations in the front part of the pile-up and therefore also destroying a possible symmetric dissolution thus leading to a more *classical* picture of dislocation storage and possibly pile-up dissolution with no forward plasticity. However, DDD simulations with much higher dislocation densities have also shown some irreversible net plastic deformation in one loading cycle [24] suggesting that the forward process should be operational in these situations as well.

In experiments, the geometric argument should also play a role in bending scenarios. No sample is perfectly shaped but rounded or tapered. However, if the geometry is thinner on the opposite side of the source, the shape asymmetry favors dislocation motion to the surface on the opposite side of the source.

For the fatigue behavior of small-scale specimens it is important to note that the net plastic deformation caused by one dislocation reaching beyond the neutral plane and subsequently moving forwards through the specimen upon unloading is a fully repeatable process. One dislocation source in the specimen must experience a sufficiently high stress to generate more than one dislocation for this process to operate. This is a necessary condition for the leading dislocation reaching beyond the neutral plane and therefore a necessary condition for irreversible plasticity. Once the forward moving dislocation has left the specimen, the remaining dislocation structure and the dislocation source do not experience any back-stress and therefore are unperturbed to generate the same amount of dislocations again in the next cycle. Since no hardening process is involved, this model suggests that small scale specimens under cyclic (bending) loading should show rather digital fatigue behavior. Below a critical stress amplitude they may just show a very limited irreversible response from the heat generated during backward and forward motion of any dislocation in the specimen [25]. At sufficiently large stress amplitudes, small scale specimens should fail within a small number of cycles since each cycle will generate at least a displacement of one Burgers vector and a few thousand cycles should thereby shear off a micrometer-sized specimen.

In conclusion, a mechanism is found, which explains how a dislocation can glide

through the entire cross-section of a single crystalline sample under cyclic loading conditions. It necessarily involves stress gradients, e.g bending or torsion and operates in the limit of very low dislocation densities. This elementary mechanism leads to unidirectional plastic deformation in cyclic loading, without dislocation storage. The formation of a pile-up of two or more dislocations is required to push dislocations within an externally imposed stress-gradient beyond the neutral plane. Upon unloading, some of these dislocations do not glide back over the neutral plane, but leave the specimen on the opposite side of the source. This irreversible forward motion may be aided by the decrease of dislocation line length due to the geometry of the specimen. An asymmetry between the forwards and backwards motion due to dislocation reactions is not required for irreversible dislocation motion in this case.

With increasing dislocation density, the mechanism described here is expected to be less effective, since dislocations on different glide systems interact and form stable junctions, leading to hardening and therefore immobilizing the dislocations before reaching the sample surface. Cross-slip is another competing mechanism increasing the irreversibility during dislocation microstructure evolution, e.g. by inhibiting screw dislocation pile-ups. Therefore, the mechanism is expected to occur preferably in materials with a low stacking fault energy, where cross-slip is more difficult. Another possibility to inhibit cross-slip, particularly in a bending scenario, is to choose a crystallographic orientation with respect to the bending axis such that the formation of a dislocation pile-up of non-screw character is favored. The presented mechanism is able to explain experimentally observed slip traces after cyclic loading, and shows that these traces occur after unloading only. It is fully repeatable in successive loading cycles.

This work was performed on the computational resource bwUniCluster funded by the Ministry of Science, Research and Arts and the Universities of the State of Baden-Württemberg, Germany, within the framework program bwHPC. The financial support for the research group FOR1650 *Dislocation based plasticity*

funded by the German Research Foundation (DFG) under contract number WE3544/5-2 is gratefully acknowledged.

[1] B. Devincre, L. Kubin, T. Hoc, Scripta Mater. 54 (2006) 741–746. doi:10.1016/j.scriptamat.2005.10.066.

[2] L. Kubin, B. Devincre, T. Hoc, Mater. Sci. Eng.: A 483484 (2008) 19–24. doi:http://dx.doi.org/10.1016/j.msea.2007.01.167, 14th International Conference on the Strength of Materials.

[3] S. Suresh, Fatigue of materials, Cambridge university press, 1998.

[4] F. Mompiou, D. Caillard, M. Legros, H. Mughrabi, Acta Mater. 60 (2012) 3402–3414. doi:10.1016/j.actamat.2012.02.049.

[5] H. Mughrabi, Acta Metall. 31 (1983) 13671379. doi:10.1016/0001-6160(83)90007-X.

[6] H. Mughrabi, Metall. Mater. Trans. B 40 (2009) 431–453. doi:10.1007/s11663-009-9240-4.

[7] H. Mughrabi, Philos. T. Roy. Soc. A 373 (2015). doi:10.1098/rsta.2014.0132.

[8] A. Shyam, W. Milligan, Acta Mater. 53 (2005) 835 – 844. doi:http://dx.doi.org/10.1016/j.actamat.2004.10.036.

[9] R. Schwaiger, G. Dehm, O. Kraft, Philos. Mag. 83 (2003) 693–710. doi:10.1080/0141861021000056690.

[10] D. Kiener, C. Motz, W. Grosinger, D. Weygand, R. Pippan, Scripta Materialia 63 (2010) 500 – 503. doi:http://dx.doi.org/10.1016/j.scriptamat.2010.05.014.

[11] C. Motz, D. Weygand, J. Senger, P. Gumbsch, Acta Mater. 56 (2008) 19421955.

[12] C. Motz, T. Schöberl, R. Pippan, Acta Mater. 53 (2005) 4269–4279. doi:10.1016/j.actamat.2005.05.036.

[13] B. Szajewski, S. Chakravarthy, W. Curtin, Acta Mater. 61 (2013) 1469 – 1477. doi:http://dx.doi.org/10.1016/j.actamat.2012.11.023.

[14] C. Kirchlechner, P. Imrich, W. Liegl, J. Pörnbacher, J.-S. Micha, O. Ulrich, C. Motz, Acta Mater. 94 (2015) 69 – 77. doi:http://dx.doi.org/10.1016/j.actamat.2015.04.029.

[15] M. G. Stout, A. D. Rollett, Metall. Trans. A 21 (1990) 3201. URL: http://dx.doi.org/10.1007/BF02647315. doi:10.1007/BF02647315.

[16] S. S. Shishvan, L. Nicola, E. Van der Giessen, J. Appl. Phys. 107 (2010). URL: http://scitation.aip.org/content/aip/journal/jap/107/9/10.1063/1.3407505. doi:http://dx.doi.org/10.1063/1.3407505.

[17] R. Kumar, F. Szkely, E. V. der Giessen, Comp. Mater. Sci. 49 (2010) 46 – 54. URL: http://www.sciencedirect.com/science/article/pii/S0927025610002314. doi:http://dx.doi.org/10.1016/j.commatsci.2010.04.018.

[18] C. Zhou, R. LeSar, Comp. Mater. Sci. 54 (2012) 350 – 355. URL: http://www.sciencedirect.com/science/article/pii/S0927025611005398. doi:http://dx.doi.org/10.1016/j.commatsci.2011.09.031.

[19] G. Dehm, C. Motz, C. Scheu, H. Clemens, P. Mayrhofer, C. Mitterer, Adv. Eng. Mater. 8 (2006) 1033–1045. doi:10.1002/adem.200600153.

[20] D. Weygand, L. H. Friedman, E. V. der Giessen, A. Needleman, Model. Simul. Mater. Sci. Eng. 10 (2002) 437468.

[21] D. Weygand, P. Gumbsch, Mater. Sci. Eng.: A 400401 (2005) 158161. doi:10.1016/j.msea.2005.03.102.

[22] D. Weygand, J. Senger, C. Motz, W. Augustin, V. Heuveline, P. Gumbsch, in: W. E. Nagel, D. B. Kröner, M. M. Resch (Eds.), High

Performance Computing in Science and Engineering '08, Springer Berlin Heidelberg, 2009, p. 507523. URL: http://dx.doi.org/10.1007/978-3-540-88303-6_36. doi:10.1007/978-3-540-88303-6_36.

[23] E. van der Giessen, A. Needleman, Model. Simul. Mater. Sci. Eng. 3 (1995) 689735.

[24] J. Senger, D. Weygand, O. Kraft, P. Gumbsch, Model. Simul. Mater. Sci. Eng. 19 (2011) 074004.

[25] Y. Cheng, E. Bitzek, D. Weygand, P. Gumbsch, Model. Simul. Mater. Sci. Eng. 18 (2010) 025006. URL: http://stacks.iop.org/0965-0393/18/i=2/a=025006.